

# Effects of Crystallinity and Impurities on the Electrical Conductivity of Li-La-Zr-O Thin Films

Joong Sun Park,<sup>a,b,\*</sup> Lei Cheng,<sup>a,c</sup> Vassilia Zorba,<sup>a</sup> Apurva Mehta,<sup>d</sup> Jordi Cabana,<sup>a,e</sup>  
Guoying Chen,<sup>a</sup> Marca M. Doeff,<sup>a</sup> Thomas J. Richardson,<sup>a</sup> Jung Hoon Park,<sup>f</sup> Ji-Won Son,<sup>g</sup>  
Wan-Shick Hong<sup>f,\*</sup>

<sup>a</sup> Environmental Energy Technologies Division, Lawrence Berkeley National Laboratory, Berkeley, CA 94720, USA

<sup>b</sup> Chemical Sciences and Engineering Division, Argonne National Laboratory, Argonne, IL 60439, USA

<sup>c</sup> Department of Material Sciences and Engineering, University of California, Berkeley, CA 94720, USA

<sup>d</sup> Stanford Synchrotron Radiation Lightsource, SLAC National Accelerator Laboratory, Menlo Park, CA 94025, USA

<sup>e</sup> Department of Chemistry, University of Illinois at Chicago, IL 60607, USA

<sup>f</sup> Department of Nano-Science and Technology, University of Seoul, Seoul, Korea

<sup>g</sup> High-Temperature Energy Materials Research Center, Korea Institute of Science and Technology, Seoul 136-791, Korea

\*Corresponding author: [parkj@anl.gov](mailto:parkj@anl.gov), [wshong@uos.ac.kr](mailto:wshong@uos.ac.kr)

## ABSTRACT

We present a study of the fabrication of thin films from a  $\text{Li}_7\text{La}_3\text{Zr}_2\text{O}_{12}$  (LLZO) target using pulsed laser deposition. The effects of substrate temperatures and impurities on electrochemical properties of the films were investigated. The thin films of Li-La-Zr-O were deposited at room temperature and higher temperatures on a variety of substrates. Deposition above  $600\text{ }^\circ\text{C}$  resulted in a mixture of cubic and tetragonal phases of LLZO, as well as a  $\text{La}_2\text{Zr}_2\text{O}_7$  impurity, and resulted in aluminum enrichment at the surface when Al-containing substrates were used. Films deposited at  $600\text{ }^\circ\text{C}$  exhibited the highest room temperature conductivity,  $1.61 \times 10^{-6}\text{ S/cm}$ . The chemical stability toward metallic lithium was also studied using X-ray photoelectron spectroscopy, which showed that the oxidation state of zirconium remained at +4 following physical contact with heated lithium metal.

## INTRODUCTION

Batteries with lithium metal anodes have significantly higher theoretical energy densities compared to lithium-ion batteries. The tendency of lithium metal to form mossy deposits or dendrites upon cycling, however, leads to potentially unsafe conditions and shortened lifetimes. The use of a solid state layer that is a lithium ion conductor but electronically insulating has been proposed as a way to improve cycle life and enable the use of Li metal in high energy batteries [1-2]. The ionic conductivities of candidate phases that are chemically stable in contact with lithium metal range from  $10^{-4}$  to  $10^{-6}$  S/cm, several orders of magnitude lower than those of non-aqueous liquid electrolytes [3-6]. As a result, the engineering strategies to enable Li metal batteries include the use of a liquid electrolyte that is insulated from the metal electrode by a solid state protective layer. This protective layer must be chemically stable against lithium metal, as well as pinhole-free and thin ( $<50\mu\text{m}$ ) to compensate for its low ionic conductivity [7].

Among the candidates of solid state ion conducting materials,  $\text{Li}_7\text{La}_3\text{Zr}_2\text{O}_{12}$  (LLZO) with the garnet structure has attracted attention because of its reported chemical stability against lithium metal and the high ionic conductivity ( $10^{-4}$ - $10^{-3}$  S/cm) of the cubic polymorph [8-10]. The tetragonally distorted form of LLZO, however, has significantly lower lithium ion conductivity [9, 11]. Thin film fabrication of garnet-type LLZO has been explored by either RF sputtering or pulsed laser deposition (PLD), with the reported room temperature ionic conductivity (typically in the range of  $10^{-7}$  S/cm) several orders of magnitude lower than that of the bulk materials [12, 13]. PLD is a technique known for its ability to preserve the target stoichiometry, but the influence of impurities arising from interactions with the

substrate and the crystallinity of films, which is affected by the deposition temperature, can have profound effects on the electrical properties [14]. Recently, Kim *et al.* fabricated epitaxial LLZO (001) and (111) thin films by PLD with cubic structures showing an enhanced lithium ion conductivity of  $10^{-5}$  S/cm at room temperature [15]. Yet, systematic studies on the effect of deposition temperature on LLZO film crystallinity and electrical properties have not been performed. Here we report studies that illustrate the effect of deposition temperature and substrate type on the structural, physical and electrochemical properties of Li-La-Zr-O thin films made by PLD. Our results indicate that thin films deposited at 600 °C on MgO (100) showed cubic and tetragonal polymorph with highest conductivity, and aluminum can react with the films when deposited on Al<sub>2</sub>O<sub>3</sub> containing substrates such as sapphire or anodized aluminum oxide (AAO).

## **EXPERIMENTAL**

### *Film Preparation*

Phase pure Li<sub>7</sub>La<sub>3</sub>Zr<sub>2</sub>O<sub>12</sub> (LLZO) powders were prepared by solid state synthesis.<sup>9</sup> Mixtures of Li<sub>2</sub>CO<sub>3</sub> (Aldrich, 99.7%), La<sub>2</sub>O<sub>3</sub> (Aldrich, 99.99%) and ZrO<sub>2</sub> (Aldrich, 99%), with a 10 mol% excess of lithium to compensate for loss during heating, were ground, cold-pressed into pellets, and then heat-treated at 1000 °C for 6 h in an alumina crucible. The pellets were ground and the particles were sieved to < 75 μm in size, then further reduced to 1 μm by attrition-milling with 2 wt% poly (vinyl butyral-co-vinyl alcohol-co-vinyl acetate) (PVB), 2 wt.% dibutylphthalate (DBT) and 2 wt.% menhaden fish oil (MFO) in isopropyl alcohol (IPA). The powders were dried, pressed into pellets, covered by an

LLZO powder bed to prevent further lithium loss during heating, and sintered at 1200 °C for 10 h.

The sintered LLZO pellets were used as PLD targets to prepare thin films on various substrates: silicon (100) wafers, polished quartz, MgO (100) (MTI Corp.), anodized aluminum oxide (AAO) (Whatman Inc.), and sapphire (MTI Corp.). Silicon wafer and polished quartz are common substrates for vacuum deposition. We used films deposited on silicon wafer for SEM imaging and the films on quartz for benchtop XRD. EIS and GI-XRD studies were performed on the films deposited on MgO (100) substrates for following reasons: MgO is an insulator and it is ideal for in-plane electrical measurement. In contrast, Si is a semiconductor whose contribution to the measurement at elevated temperature may not be trivial. Reactivity of Al<sub>2</sub>O<sub>3</sub> with LLZO is well known. As mentioned in the Ref 16, aluminum can easily migrate in garnet-type LLZO which makes aluminum containing substrates (AAO and sapphire) ideal for understanding the effects of substrates during thin film fabrication. Single crystalline Al<sub>2</sub>O<sub>3</sub>, i.e. sapphire, provided smooth surfaces for deposition while AAO has practical advantages in fabricating hybrid type batteries where it allows liquid electrolyte fill pores in order to contact with solid state electrolyte one end [J. Reinacher, *Thin films of lithium ion conducting garnets and their properties*, Ph.D. thesis, Justus-Liebig-Universität Gießen, Germany, 2014]. A Lambda Physik 248 nm KrF excimer laser delivering 1.5 J/cm<sup>2</sup> was used to ablate the PLD target under 10 mtorr of oxygen with a pulse frequency of 10 Hz. The target-to-sample distance was 50 mm, and depositions were performed at room temperature, at 600 °C and at 750 °C. Typical film thicknesses were 100-200 nm. To study Al migration from Al containing substrates (AAO and sapphire) during PLD deposition, a target was prepared by sintering an LLZO powder

compact containing 6 mol % Al<sub>2</sub>O<sub>3</sub> at 1000 °C for 5 h. The cubic symmetry of the target material was confirmed by X-ray diffraction. Films made from this target were deposited at room temperature and 700 °C, respectively. 1 μm-thick films were obtained in an hour at a laser fluence of 3 J/cm<sup>2</sup>, under 50 mtorr of oxygen, pulsed at 10 Hz.

### *Sample Characterization*

X-ray diffraction (XRD) was performed using a Bruker D2 Phaser instrument (Cu Kα with  $\lambda=1.5406 \text{ \AA}$ ) to analyze the crystal structure and the crystallinity of the PLD targets as well as the fabricated films on quartz substrates. Grazing incidence XRD (GIXRD) experiments were performed to investigate depth dependent structure of the films deposited at room temperature, 600°C, and 750°C on MgO (100) substrates at Beamline 2-1 at the Stanford Synchrotron Radiation Lightsource (SSRL), using an incident photon energy of 8.0 keV (corresponding to  $\lambda=1.549 \text{ \AA}$ ). The scan rate and step size were 0.8°/min and 0.1° respectively.

Cross-sections of the films were obtained by polishing fractured samples with an Ar<sup>+</sup> ion beam (JEOL IB-19500 Cross Section Polisher) operating at 120 μA and 5 kV. The polished samples were investigated by scanning electron microscopy (SEM) using a JEOL-7500 field emission microscope. Compositional analysis of the film was performed by energy dispersive X-ray spectroscopy (EDS) with an incident beam energy of 15 kV, monitoring the K lines of Al and O, and the L lines of Zr and La. The film composition was also analyzed by femtosecond laser-induced breakdown spectroscopy (LIBS). A frequency tripled (343 nm) diode-pumped ytterbium femtosecond laser (s-pulse, Amplitude Systems) was used as the excitation source, delivering 500 fs pulses at a repetition rate of 1 Hz (pulse

energy of 150  $\mu\text{J}$ ). The fs-laser beam was focused on the sample surface by a UV microscope objective lens. Neutral density filters were used to attenuate the fs-laser beam and control the exact amount of laser energy. The laser-induced plasma optical emission was imaged onto an optical fiber bundle by UV fused silica plano-convex lenses, and the fiber was directly connected to the slit entrance of a Czerny-Turner spectrometer (1200 gr/mm)/ICCD (Acton 2150/Princeton Instruments) camera system. The gate of the ICCD camera was triggered by the fs-laser and the relative delay was controlled by the ICCD. The average composition of the LLZO PLD target was analyzed by ICP-OES (inductively coupled plasma-optical emission spectroscopy) and served as a calibration standard for quantitative LIBS determination of the atomic ratios in the thin films. The PLD target and the Li-La-Zr-O thin film deposited on a silicon wafer were analyzed under the same LIBS focusing, energy and signal collection conditions. The total composition of the thin film was acquired by LIBS signal accumulation from the surface down to the thin film/substrate interface. The Si emission signal from the substrate was also monitored to determine the location of the interface. The atomic lines of Li I (460.28, 460.29 nm), La II (433.37 nm), and Zr I (468.78 nm) were used for the analysis.

A scanning X-ray photoelectron spectroscopy (XPS) Microprobe (PHI VersaProbe) was used to determine the chemical shift of the transition metals in the ceramic samples. The experiments were carried out with monochromatized Al  $K\alpha$  radiation (1486 eV) and a 0.05 eV energy step. A Li-La-Zr-O thin film or 100  $\mu\text{m}$  thick Ohara lithium ion conducting glass-ceramic plate ( $\text{Li}_{1+x+y}\text{Al}_x\text{Ti}_{2-x}\text{Si}_y\text{P}_{3-y}\text{O}_{12}$ , <http://www.oharacorp.com>) was pressed against a piece of lithium metal in an Ar-filled glovebox and heated at 90°C for 15 hrs. The lithium was then peeled off, and the ceramics were analyzed by XPS, at the Zr 3d and

Ti 2p levels for the Li-La-Zr-O thin film on the silicon wafer and the Ohara glass-ceramic, respectively. For comparison, XPS spectra of the pristine ceramics were also collected using the same conditions.

The electrical properties of the thin films were measured by electrochemical impedance spectroscopy (EIS) using a Gamry Potentiostat (FAS2, Gamry Instruments, Inc). Conductivity measurements were carried out on films deposited on an insulating substrate MgO (100) (1 cm×1 cm). Dense 100 nm thick platinum pads (750 μm×750 μm, 350 μm apart) were deposited on the thin film by DC sputtering. AC impedance measurements were conducted in ambient air from 300 kHz to 0.1 Hz with an amplitude of 50 mV, over the temperature range 175 to 375°C. To investigate chemical stability in a humidified environment, some films were kept in a small container in the presence of a water-filled beaker before electrochemical characterization.

## **RESULTS AND DISCUSSION**

The XRD patterns of the PLD target and the Li-La-Zr-O thin film prepared at room temperature are shown in Figure 1-(a). The PLD target exhibited a cubic phase garnet-type structure with minor impurities identified as  $\text{La}_2\text{Zr}_2\text{O}_7$  and  $\text{LiAlO}_2$ , the latter presumably arising from interaction with the alumina crucible. The as-deposited Li-La-Zr-O thin film on quartz showed only a broad XRD feature between 15 and 30°  $2\theta$ , indicating that the film was amorphous. The composition of the film was analyzed using femtosecond LIBS, which is very sensitive to lithium content. Figure 1-(b) shows the LIBS spectra for the PLD target (black) and the thin film Li-La-Zr-O (red). Elemental atomic ratios for Li, La, and Zr were

obtained using spectral line integration, and oxygen contents were calculated based on charge neutrality assumptions. The composition of the thin film was  $\text{Li}_{4.79}\text{La}_3\text{Zr}_{1.92}\text{O}_{10.75}$  (normalized to La), lower in lithium than the target ( $\text{Li}_{6.19}\text{La}_3\text{Zr}_{1.93}\text{O}_{11.46}$ ), indicating that some lithium (and possibly oxygen) was lost during the deposition process. An SEM cross-section image of the Li-La-Zr-O thin film deposited on a silicon substrate is shown in Figure 1-(c). The 200 nm thick film was dense, and generally had a smooth surface without visible signs of the micron size droplets that sometimes form during laser deposition [15].

To improve the crystallinity of the films, the MgO (100) substrates were heated to 600 or 750 °C during film deposition. Grazing-incidence synchrotron XRD (GIXRD) was employed to monitor the structure as a function of depth. Figure 2 shows GIXRD patterns of the samples, obtained at two different incident angles: 0.25° and 2.0°. Assuming a material density of 5.107 g/cm<sup>3</sup> [9], the beam probes a depth of less than 5 nm at an incident angle of 0.25°. As shown in Figure 2-(a), all three films showed evidence of crystallinity at this very shallow depth. In addition to peaks attributed to a mixture of cubic and tetragonal garnet phases, the room temperature sample exhibits a broad impurity peak between 25 and 35° ( $2\theta$ ). This broad feature was better resolved and more intense in the sample made at 750°C and the peaks matched the main LLZO reflections except for those assigned to  $\text{La}_2\text{Zr}_2\text{O}_7$  (a common impurity encountered during synthesis of LLZO) [16]. The presence of this impurity is consistent with the overall lithium deficiencies of the films compared to the target.

At an incident angle of 2°, which corresponds to a probing depth of ~300 nm, only a minor peak around  $2\theta = 17^\circ$  and a broad feature between 25 and 35° were observed, indicating

that the films deposited at room temperature and 600°C were poorly crystalline (Figure 2-(b)). As with the patterns collected at shallower depths, a stronger, sharper peak arising from the  $\text{La}_2\text{Zr}_2\text{O}_7$  impurity was observed in the film prepared at 750°C. From these results, it appears that thin crystalline layers of a cubic and tetragonal garnet mixture formed on the surface of a primarily amorphous film in the samples deposited at room temperature and 600°C, but a  $\text{La}_2\text{Zr}_2\text{O}_7$  impurity phase becomes very prominent during higher temperature depositions, likely due to severe lithium loss during the process.

In addition to the evolution of the  $\text{La}_2\text{Zr}_2\text{O}_7$  impurity phase at high temperature, we found that, if present, aluminum in the substrate can migrate into the film. This was more pronounced during deposition at an elevated temperature. Figure 3 shows an SEM image of the polished cross section of a film deposited at 700°C on an AAO substrate. The film was divided into two distinct regions with different contrast, indicating that the composition is non-uniform. An EDS scan along the dotted line in Figure 3 revealed that the upper region of the film was rich in aluminum and oxygen. Notably, the aluminum counts in this region were comparable to the substrate. The driving force for the segregation of aluminum near the film surface is not clear at this point. A plausible mechanism may involve the existence of a driving force for aluminum migration through the film, in part provided by its reaction with a source of lithium at the film surface, arising either from the target or the reactor. Such rapid diffusion of aluminum from a substrate, through a film to form an impurity layer on the surface of the film has been observed previously [17]. Chamber atmospheres enriched with impurities and the resulting incidental modification of deposited films are commonly observed in plasma deposition systems containing volatile species such as phosphorus or sulfur [18].

AC impedance measurements were carried out to determine the conductivities of the Li-La-Zr-O thin films deposited at room temperature, 600°C, and 750°C on MgO (100) substrates. Between 175 and 375 °C, the frequency dispersion showed a single depressed semicircle and a tail with an angle of about 45° at lower frequencies (Figure 4-(a)), as reported earlier for thin films of different phases, measured in a similar geometric configuration [19-21]. This is indicative of the presence of conduction carriers in the films. The Nyquist plot was fitted assuming a parallel connection of a resistor and a constant phase element (CPE). The electronic conductivity of the garnet LLZO has been shown to be four orders of magnitude lower than the ionic conductivity [8, 22, 23], so that the conductivity of the thin film was assumed to be primarily ionic. Arrhenius plots for the total electrical conductivities of the Li-La-Zr-O thin film samples deposited at different temperatures are shown in Figure 4-(b). The activation energy determined from a linear fit to the Arrhenius equation for the films deposited at room temperature was 0.41 eV, similar to values reported for  $\text{Li}_7\text{La}_3\text{Zr}_2\text{O}_{12}$  with the tetragonal structure, which range from 0.41eV-0.67eV [22, 23]. An activation energy of 0.35 eV was obtained for the films deposited at 600°C, closer to 0.30 eV, the reported value for cubic  $\text{Li}_7\text{La}_3\text{Zr}_2\text{O}_{12}$  [8-10]. These films also showed 1.5-2 times higher electrical conductivity than the room temperature deposited film, possibly due to their greater crystallinity. Increasing the PLD deposition temperature to 750°C, which led to formation of  $\text{La}_2\text{Zr}_2\text{O}_7$ , resulted in a higher activation energy of 0.67 eV, and a decrease in the conductivity of two to three orders of magnitude, as expected from the presence of an insulating phase in the layer. The room temperature conductivity of the film deposited at 600°C was extrapolated from the Arrhenius relation and found to be  $1.61 \times 10^{-6}$  S/cm, comparable to values found for tetragonal LLZO. The conductivity of

samples kept in humidified environments showed little difference, indicating that proton involvement in the conduction of the Li-La-Zr-O thin films can be considered negligible. The area specific resistance (ASR) was calculated to be only 12.4 Ohm·cm<sup>2</sup> at room temperature, in spite of the relatively low conductivity. Because the films are so thin, the ohmic losses from ion transport are very small, implying that they could be viable as a protective layer in an electrochemical cell, provided that they are pinhole free and sufficiently robust under operating conditions.

The chemical stability of the thin films was investigated using XPS. Previous reports suggested high stability of Li<sub>7</sub>La<sub>3</sub>Zr<sub>2</sub>O<sub>12</sub> against Li metal, but the evidence was indirect as the studies were performed either by visually inspecting for color changes after exposure<sup>5</sup> or using bulk techniques that are not surface sensitive [16]. Since the reactions between the solid electrolyte and Li are interfacial in nature, it is possible that a reaction occurs, such as reduction of Zr, but it is not extensive enough to be detected. For this purpose, a piece of lithium foil was pressed onto the thin film deposited at room temperature and the assembly was heated at 90 °C for 15 h. For comparison, a 100 μm thick Ohara glass-ceramic plate (Li<sub>1+x+y</sub>Al<sub>x</sub>Ti<sub>2-x</sub>Si<sub>y</sub>P<sub>3-y</sub>O<sub>12</sub>) was treated similarly. This material is known to be unstable with respect to reduction by metallic lithium [24]. Figure 5-(a) shows the high-resolution Ti spectra from the pristine and Li-treated Ohara glass-ceramic. The Ti 2p<sub>3/2</sub> peak around 459 eV is attributed to Ti<sup>4+</sup>. A shoulder at 458 eV was observed on the glass-ceramic after contact with lithium at 90 °C, indicating that Ti<sup>4+</sup> was reduced to Ti<sup>3+</sup> by lithium metal under these conditions. In addition, the color of the sample changed from white to black, a visual indicator of the instability of the glass toward lithium metal. In contrast, there was no change in color for the Li-La-Zr-O film after contact with heated

lithium. Comparison of the spectra in figure 5-(b) revealed there was no change in the Zr  $3d_{3/2}$  and  $3d_{5/2}$  levels for the Li-La-Zr-O thin film after contact with lithium, indicative of the fact that  $Zr^{4+}$  was not reduced to  $Zr^{3+}$  [25], which, in turn, suggests the film was more stable than the Ohara glass sample.

## **CONCLUSION**

We have fabricated dense and continuous Li-La-Zr-O thin films by PLD at various temperatures and investigated their physical properties. Compositions, structures, and electrical conductivities of the films were highly sensitive to deposition temperature and substrate type. Samples deposited at  $600^{\circ}\text{C}$  contained both cubic and tetragonal polymorphs of LLZO at the surface and had the highest conductivities, estimated to be  $1.61 \times 10^{-6}$  S/cm at room temperature. Because these films are very thin, their area specific resistance is low. Combined with low reactivity with metallic lithium, Li-La-Zr-O films made by PLD may be suitable for use as protective ion conducting layers in lithium metal batteries.

## **ACKNOWLEDGEMENTS**

This work was supported by the Assistant Secretary for Energy Efficiency and Renewable Energy, Office of Vehicle Technologies and the Chemical Sciences, Geosciences, and Biosciences Division, Office of Basic Energy Sciences of the U.S. Department of Energy under contract no. DE-AC02-05CH11231. A portion of this work was done at Stanford

Synchrotron Radiation Lightsource, SLAC National Accelerator Laboratory, which is supported by the U.S. Department of Energy, Office of Science, Office of Basic Energy Sciences under Contract No. DE-AC02-76SF00515.

This document was prepared as an account of work sponsored by the United States Government. While this document is believed to contain correct information, neither the United States Government nor any agency thereof, nor the Regents of the University of California, nor any of their employees, makes any warranty, express or implied, or assumes any legal responsibility for the accuracy, completeness, or usefulness of any information, apparatus, product, or process disclosed, or represents that its use would not infringe privately owned rights. Reference herein to any specific commercial product, process, or service by its trade name, trademark, manufacturer, or otherwise, does not necessarily constitute or imply its endorsement, recommendation, or favoring by the United States Government or any agency thereof, or the Regents of the University of California. The views and opinions of authors expressed herein do not necessarily state or reflect those of the United States Government or any agency thereof or the Regents of the University of California.

## REFERENCES

1. M. Y. Chu, S. Visco, L.C. De Jonghe, Plating metal negative electrodes under protective coatings, U.S. Patent No. 6402795 (2002)
2. P. G. Bruce, S. A. Freunberger, L. J. Hardwick, J-M. Tarascon, Li-O<sub>2</sub> and Li-S batteries with high energy storage, *Nat. Mat.* 11 (2012) 19.
3. P. Knauth, Inorganic solid Li ion conductors: An overview, *Solid State Ionics* 180 (2009) 911.
4. T. Minami, A. Hayashi, M. Tatsumisago, Recent progress of glass and glass-ceramics as solid electrolytes for lithium secondary batteries, *Solid State Ionics* 180 (2006) 2715.
5. N.J. Dudney, Addition of a thin-film inorganic solid electrolyte (Lipon) as a protective film in lithium batteries with a liquid electrolyte, *J. Power Sources.* 89 (2000) 176.
6. L. Zhang, L. Cheng, J. Cabana, G. Chen, M. M. Doeff, T. J. Richardson, Effect of lithium borate addition on the physical and electrochemical properties of the lithium ion conductor  $\text{Li}_{3.4}\text{Si}_{0.4}\text{P}_{0.6}\text{O}_4$ , *Solid State Ionics* 231 (2013) 109.
7. J. Christensen, P. Albertus, R. S. Sanchez-Carrera, T. Lohmann, B. Kozinsky, R. Liedtke, J. Ahmed, A. Kojic, A critical review of Li/air batteries, *J. Electrochem. Soc.* 159 (2012) R1.
8. R. Murugan, V. Thangadurai, W. Weppner, Fast lithium ion conduction in garnet-type  $\text{Li}_7\text{La}_3\text{Zr}_2\text{O}_{12}$ , *Angew. Chem. Int. Ed.* 46 (2007) 7778.
9. C. A. Geiger, E. Alekseev; B. Lazic, M. Fisch, T. Armbruster, R. Langner, M. Fechtelkord, N. Kim, T. Pettke, W. Weppner, Crystal chemistry and stability of " $\text{Li}_7\text{La}_3\text{Zr}_2\text{O}_{12}$ " garnet: a fast lithium-ion conductor, *Inorg. Chem.* 50 (2011) 1089.

10. L. Cheng, J. S. Park, H. Hou, V. Zorba, G. Chen, T. Richardson, J. Cabana, R. Russo, M. Doeff, Effect of microstructure and surface impurity segregation on the electrical and electrochemical properties of dense Al-substituted  $\text{Li}_7\text{La}_3\text{Zr}_2\text{O}_{12}$ , *J. Mater. Chem. A* 2 (2014) 172.
11. J. Awaka, N. Kijima, H. Hayakawa, J. Akimoto, Synthesis and structure analysis of tetragonal  $\text{Li}_7\text{La}_3\text{Zr}_2\text{O}_{12}$  with the garnet-related type structure, *J. Solid State Chem.* 182 (2009) 2046.
12. J. Tan, A. Tiwari, Fabrication and characterization of  $\text{Li}_7\text{La}_3\text{Zr}_2\text{O}_{12}$  thin films for lithium ion battery, *ECS Solid State Letters*, 1 (2012) Q57.
13. D. J. Kalita, S. H. Lee, K. S. Lee, D. H. Ko, Y. S. Yoon, Ionic conductivity properties of amorphous Li–La–Zr–O solid electrolyte for thin film batteries, *Solid State Ionics* 229 (2012) 14.
14. D. B. Chrisey, G. K. Hubler, *Pulsed Laser Deposition of Thin Films*, Wiley, New York, 1994
15. S. Kim, M. Hirayama, S. Taminato, R. Kanno, Epitaxial growth and lithium ion conductivity of lithium-oxide garnet for an all solid-state battery electrolyte, *Dalton Trans.* 42 (2013) 13112.
16. M. Kotobuki, K. Kanamura, Y. Sato, T. Yoshida, Fabrication of all-solid-state lithium battery with lithium metal anode using  $\text{Al}_2\text{O}_3$ -added  $\text{Li}_7\text{La}_3\text{Zr}_2\text{O}_{12}$  solid electrolyte, *J. Power Source* 196 (2011) 7750.
17. J. H. Ahn, S. Park, J. Lee, Y. Park, and J-H. Lee, Local impedance spectroscopic and microstructural analyses of Al-in-diffused  $\text{Li}_7\text{La}_3\text{Zr}_2\text{O}_{12}$ , *J. Power Source* 254 (2014) 287.

18. J. R. Petherbridge, P. W. May, G. M. Fuge, K. N. Rosser, M. N. R. Ashfold, *In situ* plasma diagnostics of the chemistry behind sulfur doping of CVD diamond films, *Diam. Relat. Mater.* 11 (2002) 301.
19. I. Kosacki, C. M. Rouleau, P. F. Bechera, J. Bentley, D. H. Lowndes, Nanoscale effects on the ionic conductivity in highly textured YSZ thin films, *Solid State Ionics* 176 (2005) 1319.
20. J. H. Shim, T. M. Gür, F. B. Prinz, Proton conduction in thin film yttrium-doped barium zirconate, *Appl. Phys. Lett.* 92 (2008) 253115.
21. J. S. Park, Y.B Kim, J. An, J. H. Shim, T. M. Gür, F. B. Prinz, Effect of cation non-stoichiometry and crystallinity on the ionic conductivity of atomic layer deposited Y:BaZrO<sub>3</sub> Films, *Thin Solid Films* 539 (2013) 166.
22. E. Rangasamy, J. Wolfenstine, J. Sakamoto, The role of Al and Li concentration on the formation of cubic garnet solid electrolyte of nominal composition Li<sub>7</sub>La<sub>3</sub>Zr<sub>2</sub>O<sub>12</sub>, *Solid State Ionics* 206 (2012) 28.
23. J. Wolfenstine, J. Ratchford, E. Rangasamy, J. Sakamoto, J. Allen, Synthesis and high Li-ion conductivity of Ga-stabilized cubic Li<sub>7</sub>La<sub>3</sub>Zr<sub>2</sub>O<sub>12</sub>, *Mater. Chem. Phys.* 134 (2012) 571.
24. W. C. West, J. F. Whitacre, J. R. Lim, Chemical stability enhancement of lithium conducting solid electrolyte plates using sputtered LiPON thin films, *J. Power Sources* 126 (2004) 134.
25. S. Manna, T. Ghoshal, S. De, Room temperature stabilized cubic zirconia nanocrystal: a giant dielectric material, *J. Phys. D: Appl. Phys.* 43 (2010) 295403.

## FIGURE CAPTIONS

Figure 1-(a): XRD patterns of a Li-La-Zr-O thin film grown on a quartz substrate prepared by pulsed laser deposition at room temperature (top) and the PLD target LLZO (bottom).

Figure 1-(b): LIBS spectra of a Li-La-Zr-O thin film deposited at room temperature (red) and reference PLD target (black).

Figure 1-(c): SEM cross-section image of a 200 nm thick Li-La-Zr-O film.

Figure 2: Synchrotron-based grazing incidence XRD patterns of the Li-La-Zr-O thin films grown at room temperature (black), 600°C (red), and 750°C (blue) at (a) 0.25 ° and (b) 2.0 °. Cubic<sup>8</sup> and tetragonal<sup>11</sup> LLZO patterns are shown for reference.

Figure 3: SEM image of a polished cross section of the Li-La-Zr-O film deposited on an AAO substrate at 700°C and the corresponding EDS profile along the indicated line.

Figure 4: (a) Nyquist plot of a thin Li-La-Zr-O film on MgO measured at 325°C by electrochemical impedance spectroscopy and (b) Arrhenius plot of the Li-La-Zr-O thin films at different PLD deposition temperatures. Room temperature (black), 600°C (red), and 750°C (blue)

Figure 5: XPS spectra of Ohara glass (top) and Li-La-Zr-O thin films (bottom) before and after contact with lithium metal at 90°C for 15 hr.

# FIGURES

Figure 1-(a)

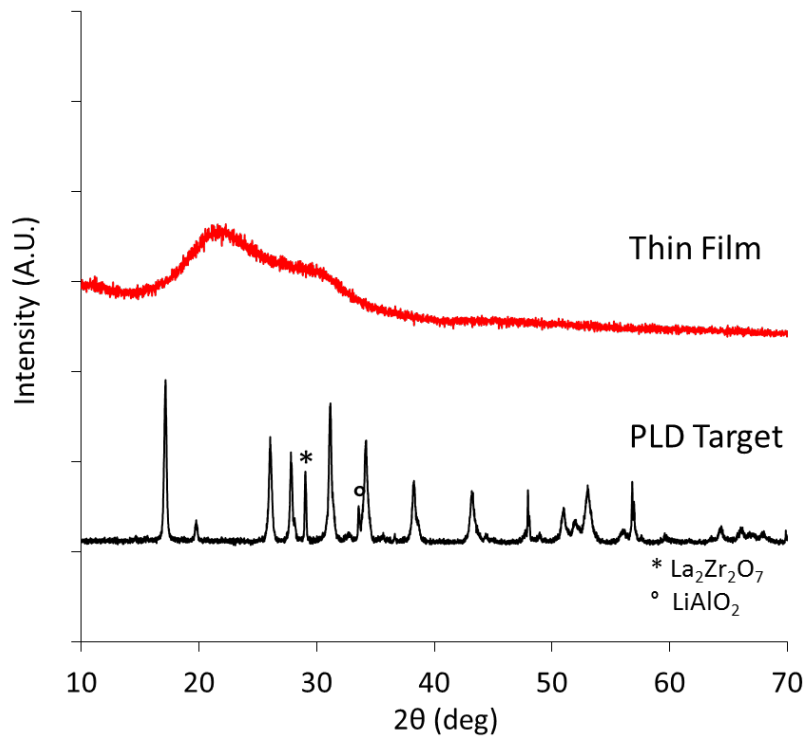


Figure 1-(b)

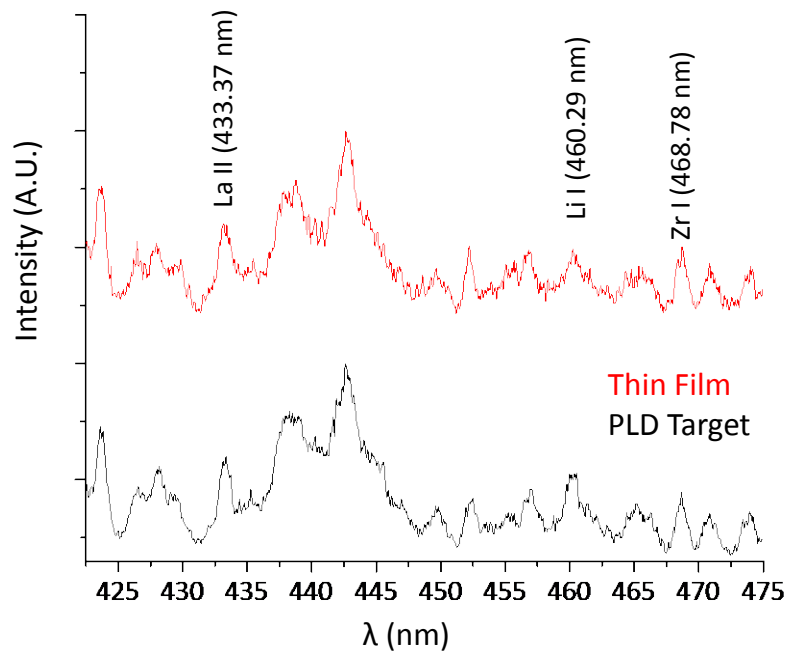


Figure 1-(c)

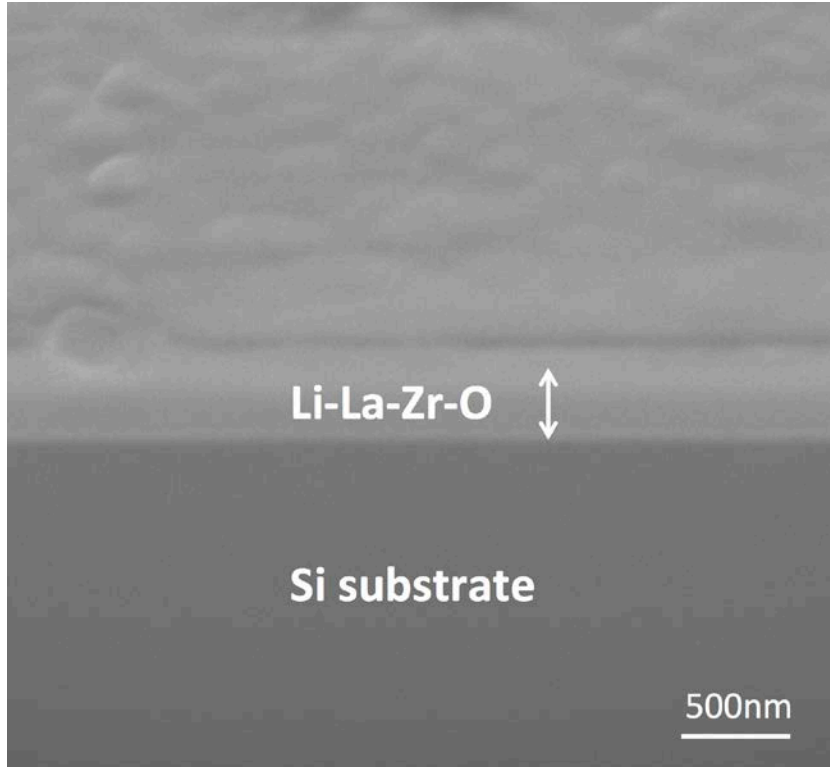


Figure 2-(a)

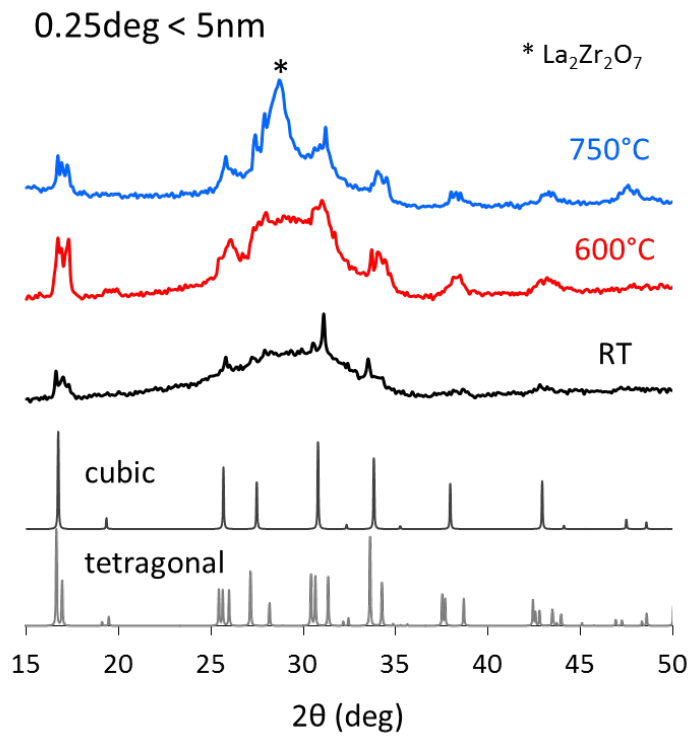


Figure 2-(b)

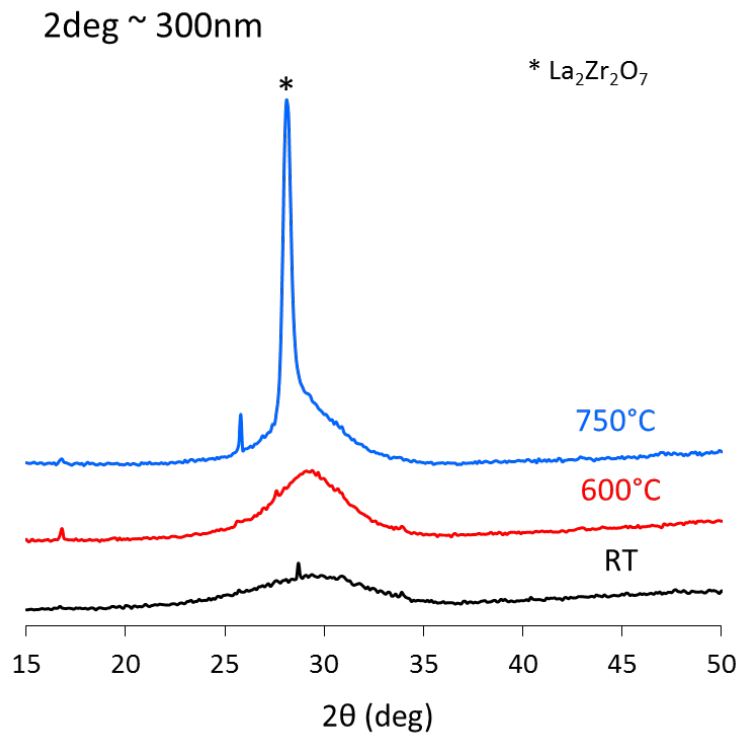


Figure 3

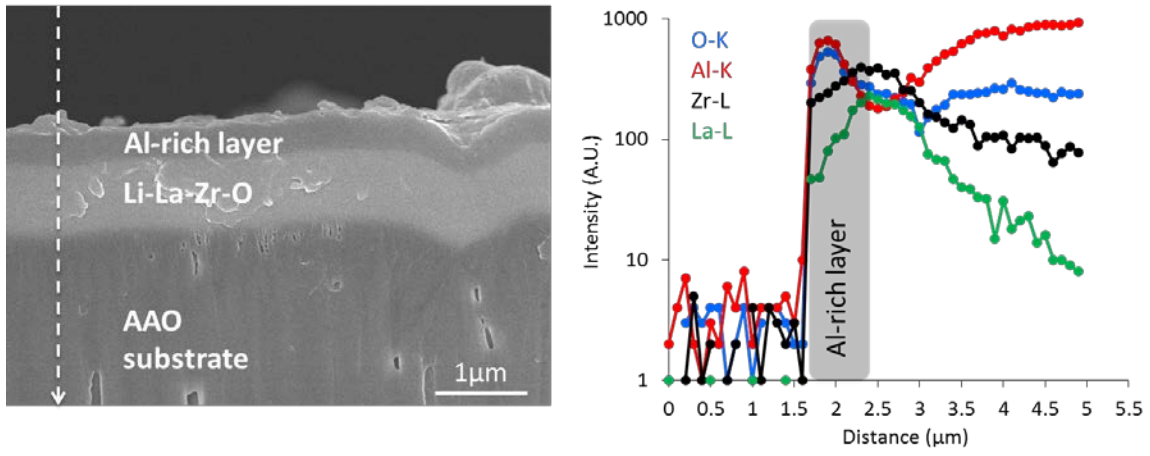


Figure 4-(a)

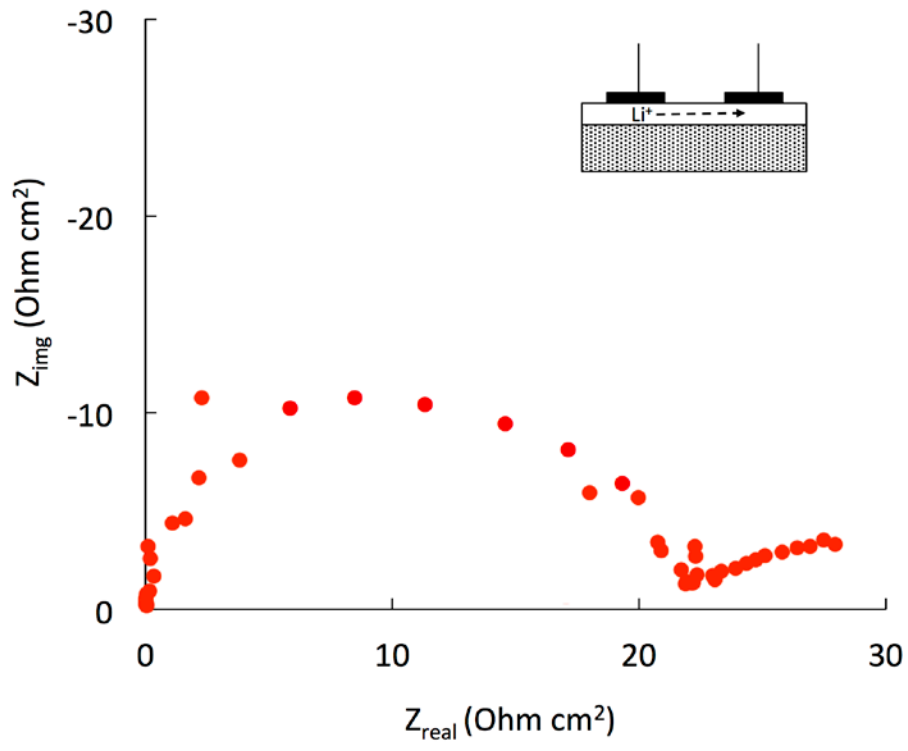


Figure 4-(b)

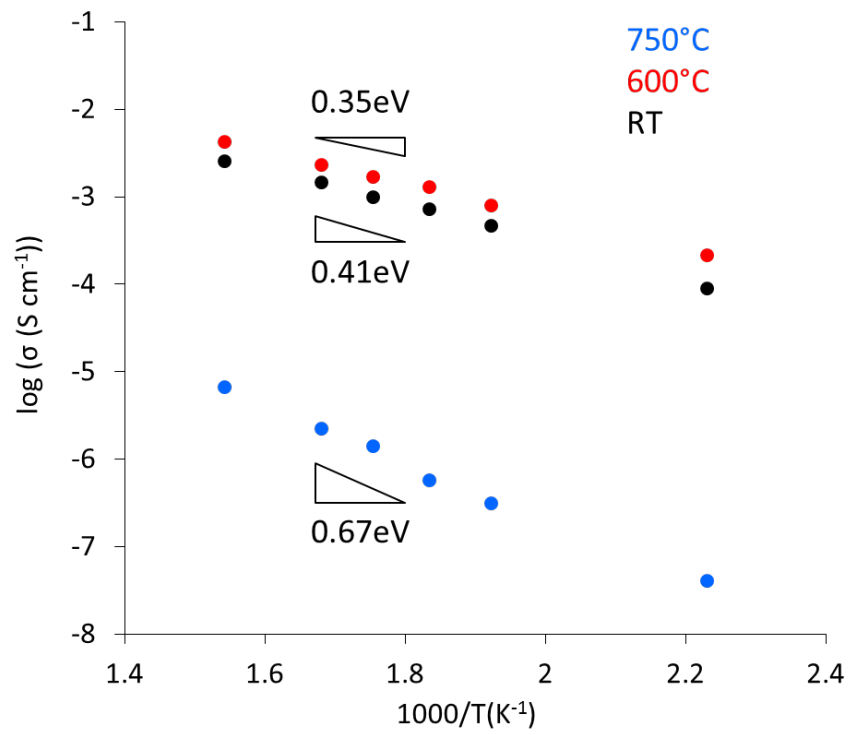


Figure 5-(a)

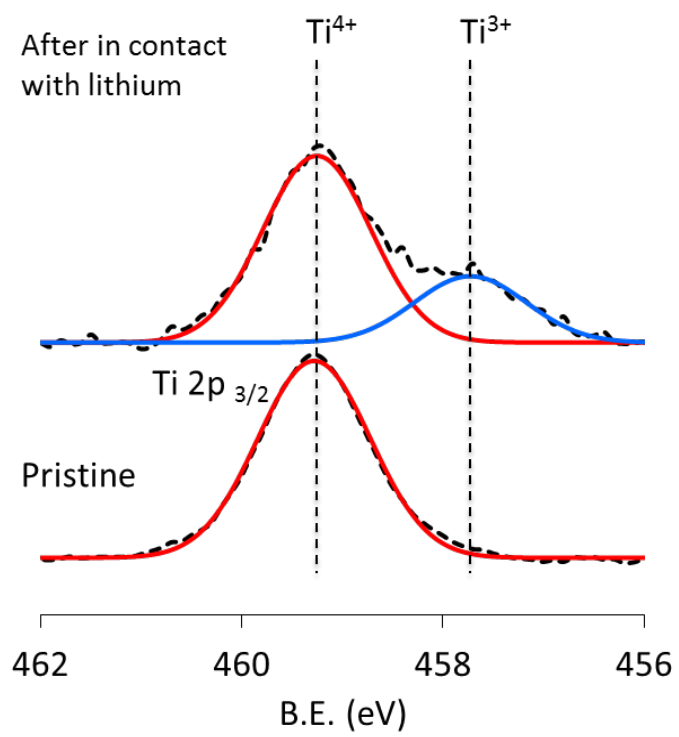


Figure 5-(b)

